Cellular/Molecular

Submillisecond Precision of the Input–Output Transformation Function Mediated by Fast Sodium Dendritic Spikes in Basal Dendrites of CA1 Pyramidal Neurons

Gal Ariav, Alon Polsky, and Jackie Schiller
Department of Physiology, Bruce Rappaport Faculty of Medicine, Technion, Haifa 31096, Israel

The ability of cortical neurons to perform temporally accurate computations has been shown to be important for encoding of information in the cortex; however, cortical neurons are expected to be imprecise temporal encoders because of the stochastic nature of synaptic transmission and ion channel gating, dendritic filtering, and background synaptic noise. Here we show for the first time that fast local spikes in basal dendrites can serve to improve the temporal precision of neuronal output. Integration of coactivated, spatially distributed synaptic inputs produces temporally imprecise output action potentials within a time window of several milliseconds. In contrast, integration of closely spaced basal inputs initiates local dendritic spikes that amplify and sharpen the summed somatic potential. In turn, these fast basal spikes allow precise timing of output action potentials with submillisecond temporal jitter over a wide range of activation intensities and background synaptic noise. Our findings indicate that fast spikes initiated in individual basal dendrites can serve as precise "timers" of output action potentials in various network activity states and thus may contribute to temporal coding in the cortex.

Key words: **dendrites; submillisecond; temporal coding; spike; cortex; synaptic integration**

Introduction

Although the manner by which information is encoded by cortical neurons is not known, there are two main theories that attempt to address this question. The rate code theory postulates that information is represented by the average firing rates of neurons, whereas the temporal code theory claims that information is conveyed by the precise timing of action potentials (Abeles, 1990; Bialek and Rieke, 1992; Rieke et al., 1997; Shadlen and Newsome, 1998; Singer, 1999; deCharms and Zador, 2000). The traditional view is that of the rate code. In recent years, however, evidence has accumulated to support the notion that the brain uses temporal coding as well. This has been demonstrated for auditory information in the brain stem (Trussell, 1999). Moreover, studies have shown that the precise timing of output action potentials can encode information in the hippocampus and neocortex as well (Richmond and Optican, 1987; Richmond et al., 1987; Softky and Koch, 1993; Hopfield, 1995; Vaadia et al., 1995; Riehle et al., 1997; Roelfsema et al., 1997; Mechler et al., 1998; Harris et al., 2002; Mehta et al., 2002).

The ability of single neurons to process and convey temporally accurate information is determined by their ability to detect coincident synaptic activity on the one hand and reliably transform this incoming synaptic activity into a temporally accurate output pattern on the other hand. Accurate input coincidence detection at the axo-somatic region is limited by passive attenuation of high-frequency signals along the dendritic tree (Rall and Segev, 1987; Magee, 2000). Dendrites contain multiple active conductances, which have been suggested to interact locally and amplify the response of synchronously activated neighboring inputs, a phenomenon termed "cluster sensitivity" by Mel (for review, see Magee et al., 1998; Mel, 1999; Hausser et al., 2000; Reyes, 2001; Schiller and Schiller, 2001; Migliore and Shepherd, 2002). These local dendritic interactions have been predicted to facilitate input coincidence detection of neighboring inputs at the activated dendritic site (Softky, 1994); however, the experimental findings reported in the literature regarding this possibility are contradictory. Although Cash and Yuste (1999) found no evidence of input coincidence detection in dendrites of CA1 pyramidal neurons, Larkum et al. (1999) reported coincidence detection of inputs arriving at different cortical layers, and Williams and Stuart (2002) recently reported that dendritic calcium spikes can serve as input coincidence detectors of large signals in apical dendrites of layer 5 pyramidal neurons. Then again, in these studies the impact of apical calcium spikes on the temporal accuracy of neuronal output was not examined; the authors measured the existence and number of axonal action potentials but not their timing or jitter.

Coincidence detection of input synaptic data is not sufficient for performing reliable temporal coding. Rather, input information must also be transformed into temporally precise output

Received Jan. 13, 2003; revised June 27, 2003; accepted June 30, 2003.

This work was supported by the German–Israeli Foundation, the Rapport Foundation, and the Minerva Foundation. We thank S. Marom, Y. Schiller, and G. Major for critically reading an earlier version of this manuscript.

Correspondence should be addressed to Dr. Jackie Schiller, Technion Medical School, Bat-Galim, Haifa 31096, Israel. E-mail: jackie@tx.technion.ac.il.

 0270-6474/03/237750-09$15.00/0

action potentials. The basic components of neurons, namely ionic channels and synapses, are relatively unreliable and behave stochastically, and the neuron is constantly bombarded by background synaptic activity. As a result, the process of action potential encoding is noisy, and repeated identical stimuli result in a jitter of action potential timing (Lecar and Nossal, 1971a,b; Bernander et al., 1991; Steinmetz et al., 2000). In general, both the dynamics of cortical networks as well as the active properties of single neurons were suggested to overcome these potential problems in neuronal output precision and contribute to precise action potential timing (Softky and Koch, 1993; Shadlen and Newsome, 1994; Softky, 1994; Mainen and Sejnowski, 1995; Marsalek et al., 1997; Stevens and Zador, 1998; Van Vreeswijk and Sompolinsky, 1998). Previous studies have shown that the accuracy of output action potential timing can be significantly improved by rapidly changing voltage swings at the soma (Mainen and Sejnowski, 1995; Stevens and Zador, 1998). Various potential mechanisms have been suggested to underlie these sharp voltage transients, including involvement of active dendritic mechanisms and synchronous synaptic input (Softky and Koch, 1993; Softky, 1994; Mainen and Sejnowski, 1995).

In the present study, we report that fast local spikes in basal dendrites can serve as efficient coincidence detectors of incoming synaptic information and as temporally stable and precise output action potential generators over a wide range of activation intensities and background noise.

Materials and Methods

Slice preparation and electrophysiological recording. Hippocampal brain slices 300–350 μm thick were prepared from 17- to 40-d-old Wistar rats. Whole-cell patch-clamp recordings were performed from visually identified CA1 pyramidal neurons using infrared-differential interference contrast optics. The extracellular solution contained (in mM): 125 NaCl, 25 $NaHCO_3$, 25 glucose, 3 KCl, 1.25 NaH_2PO_4, 2 $CaCl_2$, 1 $MgCl_2$, pH 7.4, at 34–35°C. Bicuculline methiodide (1 μM) was added to the extracellular solution in most experiments. The intracellular solution contained (in mM): 115 K^+-gluconate, 20 KCl, 2 Mg-ATP, 2 Na_2-ATP, 10 Na_2-phosphocreatine, 0.3 GTP, 10 HEPES, 0.15 Calcium Green-1 (CG-1), or 0.2 Oregon Green 488 Bapta-1 (OGB-1), pH 7.2. The electrophysiological recordings were performed using Multi-Clamp 700A (Axon Instruments, Foster City, CA), and the data were acquired and analyzed using PClamp 8.2 (Axon Instruments) and Igor (Wavemetrics, Lake Oswego, OR) software. The average values are presented as average ± SD, and statistical analysis was performed using the Student's *t* test.

Focal synaptic stimulation and calcium fluorescence imaging. Focal synaptic stimulation was performed via a theta patch pipette located in close proximity to the selected basal dendritic segment guided by the fluorescent image of the dendrite (Schiller et al., 2000). In these experiments, the neurons were filled with the calcium-sensitive dye, and the basal dendritic tree was imaged with a confocal imaging system (Olympus Fluoview) mounted on an upright BX51WI Olympus microscope (Tokyo, Japan) equipped with a 60× (Olympus, 0.9 numerical aperture) water objective. Full images were obtained with a temporal resolution of 1 Hz, and line scan images were obtained with a temporal resolution of 512 Hz. Images were analyzed using Tiempo (Olympus) and Igor software. When apical and basal inputs were paired, spikes and EPSPs were produced either synaptically or by injected somatic waveforms. The injected current waveforms were obtained by playing back the recorded voltage waveforms in a model CA1 using the NEURON software (Hines and Carnevale, 1997). Synaptic basal and apical EPSPs were evoked by monopolar synaptic stimulation to allow for distributed activation of inputs and avoid focal synaptic stimulation. In all cases, distributed synaptic activation met two criteria. First, a linear stimulus response curve was observed. Second, no focal rise in dendritic calcium transient could be identified. Despite compliance with these criteria, we could not rule out that there was a small voltage contribution caused by focal interaction of arbitrarily activated closely spaced inputs. Fast basal spikes were evoked by focal synaptic stimulation of an identified basal branch.

Glutamate uncaging. For the uncaging experiments, caged glutamate (γ-ANB-caged L-glutamic acid) (Molecular Probes, Eugene, OR) was photolyzed by a 361 nm UV–laser beam (Innova 300, Coherent, Palo Alto, CA) using 1 msec shuttered pulses (UniBlitz shutter driver/timer, Rochester, NY). After a stable whole-cell recording was established, the recording chamber was perfused with extracellular solution (bubbled with 95% O_2/5% CO_2) containing freshly prepared caged glutamate compound (1 mM). The full width at half-maximum size of the photolyzed spot was 6.5 ± 3 μm in brain slices, as measured by caged fluorescein dextran (dextran DMNB-caged fluorescein; Molecular Probes).

Computer simulations. Computer simulations were performed using the compartmental modeling package NEURON on a Pentium PC under Windows XP (Hines and Carnevale, 1997). Simulations were performed on a reconstructed CA1 pyramidal neuron containing 417 dendritic segments. In addition, a 400-μm-long axon, broken into seven compartments, was appended to the soma. No special hillock morphology in the axon was used. The neuron was reconstructed and courteously provided by Dr. Guy Major (Princeton University, Princeton, NJ). The membrane resistance (R_m), cytoplasmic resistance (R_i), and membrane capacitance (C_m) were set to 16,000 Ω/cm^2, 150 Ω/cm, and 1 $\mu F/cm^2$, respectively. Other passive biophysical parameters of the model are as follows: $E_{leak} = -80$ mV, $E_{Na} = 50$ mV, $E_K = 87$ mV, and $E_{Ca} = 130$ mV. The temperature used in all experiments was 36°C.

Spines were accounted for by decreasing the R_m and increasing C_m by a factor of 2, starting 100 μm from the soma in the apical tree and 20 μm in the basal tree.

The parameters for the voltage-gated and synaptic conductances were on the basis of published experimental and modeling work (Destexhe et al., 1994; Colbert et al., 1997; Hoffman et al., 1997; Magee, 1998). The membrane of basal dendrites in the model cell contained fast voltage-gated sodium channels (200 $pS/\mu m^2$); voltage-gated calcium channels of the L (6 $pS/\mu m^2$), T (3 $pS/\mu m^2$), Q, R, and N (2 $pS/\mu m^2$ each) subtypes; voltage-gated potassium channels of the DR (5–10 $pS/\mu m^2$), and A (15 $pS/\mu m^2$) subtypes; H channels (15 $pS/\mu m^2$); and calcium activated potassium channels (2 $pS/\mu m^2$). A modified Hodgkin-Huxley scheme was used for voltage-gated conductances. The excitatory synaptic inputs were composed of AMPA (1 ± 0.2 nS) and NMDA (0.3 nS) conductances. Inhibitory GABA-A conductance was 0.5 nS. The basal fast spike was either produced by five closely spaced synaptic inputs or by a single input with AMPA (3 nS) and NMDA (5 nS) conductances that were located at 150–200 μm from the soma. Neuron files can be obtained from J.S. (jackie@tx.technion.ac.il).

Results

To reveal the contribution of active dendritic conductances to the kinetics and amplitude of summed synaptic potentials, we activated inputs clustered onto a dendritic compartment, where interactions are expected to be maximal (Shepherd and Brayton, 1987; Mel, 1999). Closely spaced inputs innervating the same basal dendrite were activated using two adjacent focal stimulating electrodes (20–40 μm apart) (Fig. 1*a*). The dendritic location of activated inputs was confirmed via concomitant calcium imaging measurements, which showed that each of the two individual EPSPs resulted in a small local dendritic $[Ca^{2+}]_i$ transient (size of the activated dendritic segment was 3–6 μm) in the stimulated basal dendrite (Schiller et al., 2000). Addition of APV and CNQX abolished altogether the EPSP and $[Ca^{2+}]_i$ transient ($n = 3$) (Fig. 2*c*). These findings eliminated the possibility of direct electrical stimulation of the dendrite.

Comparison of the individual, small EPSPs evoked by each electrode with the summed EPSP evoked by coincident activation of both electrodes revealed that the summed EPSP was much faster than expected (Fig. 1*b*). The rise time of the individual small EPSPs could be fitted by a monoexponential function with an average time constant of 3.02 ± 1.19 msec ($n = 25$). In con-

trast, the rising phase of summed EPSPs showed a second fast regenerative component that could be fitted with a time constant of 0.31 ± 0.13 msec (Fig. 1*b*) ($n = 22$; $p < 0.0001$ as compared with the individual EPSPs).

Coincident activation of the two adjacent electrodes also resulted in supralinear amplification of the summed potential (Fig. 1*b*). The average peak amplitude of the summed potential was 1.87 ± 0.7 times larger than that of the arithmetic sum of the two individual EPSPs ($n = 12$). This result was even more pronounced for the area under the curve, which was 2.52 ± 1.09-fold larger than that expected from the arithmetic sum. Supralinear amplification was observed throughout the entire length of basal dendrites aside from the proximal 50 μm adjacent to the soma.

To determine the time window for coincidence detection of the incoming neighboring basal inputs, the individual EPSPs were activated with different time delays. Sharpening and supralinear amplification of the summed EPSP was highly dependent on the time interval between the two activated inputs. It occurred reliably when this interval was <3 msec and intermittently (25–50% of trials) at time intervals of 3–5 msec ($n = 4$) (Fig. 1*c*). When the time interval between the activated inputs was >5 msec, individual EPSPs summated linearly or sublinearly, and the regenerative response was absent. It should be noted that in our experimental conditions each EPSP is a sum of several synchronously activated inputs, and thus we probably overestimated the time window required for coincidence detection. Taken together these findings indicated that basal dendrites could serve as efficient coincident detectors of synaptic inputs innervating the same dendritic compartment, by both sharpening and amplifying the summed synaptic potentials as recorded at the soma.

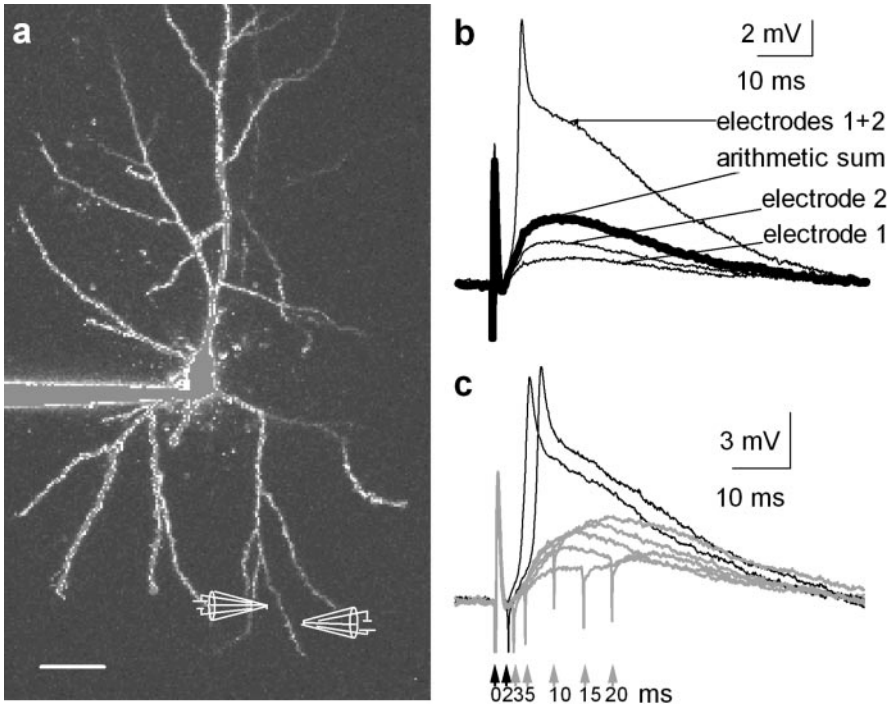

Figure 1. Rise time sharpening and supralinear amplitude amplification of the summed synaptic potential after coincident activation of synaptic inputs innervating the same dendritic branch. *a*, Fluorescent image of a CA1 pyramidal neuron loaded with OGB-1 (200 μM) via the somatic patch electrode. Two bipolar theta synaptic stimulating electrodes were placed in close proximity to a basal dendrite. Scale bar, 40 μm. *b*, Traces showing the individual EPSPs evoked by each of the synaptic stimulating electrodes, the summed synaptic potential during coincident activation of the two synaptic stimulating electrodes, and the arithmetic sum of the two individual responses (bold line). Note the large supralinear amplification and sharpening of the summed synaptic potential, as compared with the expected arithmetic sum response. *c*, Voltage traces obtained in response to coincident activation of two closely spaced electrodes at various time delays (0–20 msec). Black traces represent voltage responses to activation of the electrodes at time delays of 0 and 2 msec. Gray traces show the responses for activation at time delays of 3, 5, 10, 15, and 20 msec. Note that, in this experiment, the time window for coincident detection was <3 msec.

The underlying mechanism responsible for sharpening and supralinear amplification of coincidently activated EPSPs innervating the same dendritic compartment was the initiation of local spikes in basal dendrites (Fig. 2*a*). These local basal spikes were observed both in the presence ($n = 32$) and absence ($n = 6$) of 1 μM extracellular bicuculline. Moreover, local spikes were recorded in three cases in which the recording pipette contained 150 μM EGTA instead of fluorescence calcium dyes. In contrast to local dendritic NMDA spikes described previously in basal dendrites of layer 5 neocortical pyramidal neurons (Schiller et al., 2000), local spikes in basal dendrites of CA1 neurons were composed of early fast and late slow components. Most spikes (27 of 38 spikes) were dominated by the early fast component. The average peak amplitudes of the fast and slow components were 10.73 ± 3.46 and 7.23 ± 2.70 mV relative to the resting membrane potential ($n = 18$); however, at times dendrites produced spikes that were predominated by the slow component, as described in layer 5 pyramidal neurons ($n = 11$).

Both the fast and slow components of local basal spikes were eliminated by 15–20 mV hyperpolarization of the somatic membrane potential (Fig. 2*b*) ($n = 4$) and bath application of the NMDA-receptor blocker APV (100 μM) (Fig. 2*c*) ($n = 6$). Moreover, both hyperpolarization and APV linearized the intensity response curves (Figs. 2*d*). In three of six experiments, fast basal spikes could be reinitiated in the presence of APV by further increasing the stimulus intensity (Fig. 2*c*). This spike was completely blocked by subsequent addition of 20 μM CNQX (Fig. 2*c*) ($n = 3$).

A previous study reported that fast spikelets in CA1 pyramidal neurons were mediated by direct axonal stimulation and axo-axonal gap junctions between adjacent CA1 neurons (Schmitz et al., 2001); however, this was not the case in the present study. Both the fast and slow components of local basal spikes were abolished by APV (100 μM) and CNQX (20 μM) (Fig. 2*c*) ($n = 4$), and persisted in the presence of the gap junction blocker carbenoxolone (Fig. 2*e*) (100 μM; $n = 3$). Moreover, local fast spikes were recorded in three neurons in which the axon was cut, leaving a small axonal stump of <25 μm, as measured by three-dimensional confocal reconstruction of the cell. In addition, laser-induced destruction of the activated basal branch eliminated the spike altogether ($n = 5$). Hence, both the fast and slow components resulted from local spikes in the activated basal dendrite, rather than axonal spikelets mediated by axo-axonal gap junctions.

We used calcium imaging experiments to define the extent of spread of local basal spikes (Fig. 2*f*). Concomitant calcium imaging revealed that basal dendritic spikes were associated with local calcium transients, which were mostly confined to the activated

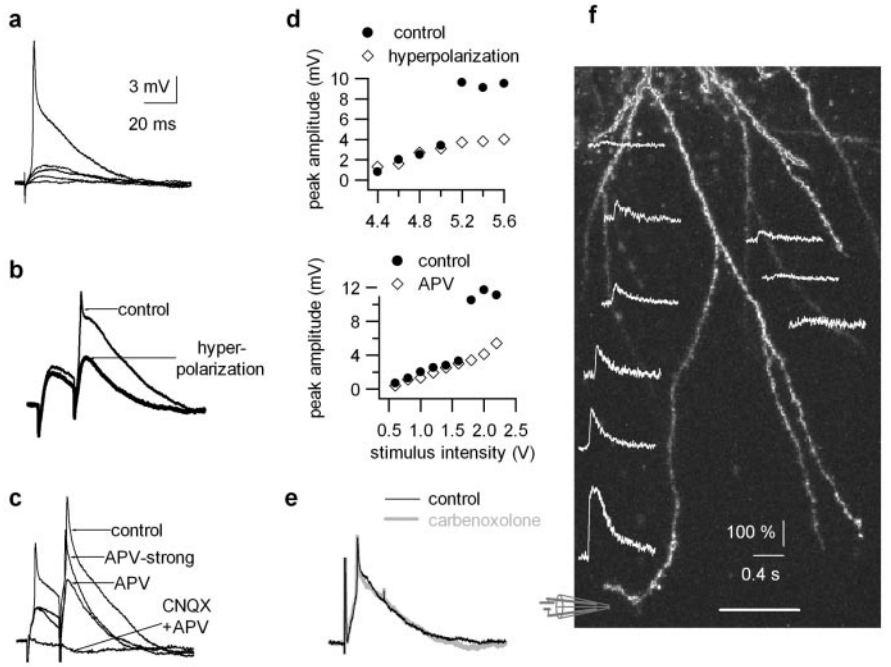

Figure 2. Synaptically evoked local spikes in basal dendrites of CA1 pyramidal neurons. *a*, Postsynaptic voltage responses were evoked by focal synaptic stimulation of a basal dendrite at increasing stimulus intensities. Note the sharp threshold of initiation of the local spike. *b*, Hyperpolarization of the membrane potential (from −64 to −80 mV) eliminated the fast and slow components of the spike. Two representative traces evoked by the same stimulus intensity (2 stimuli at 50 Hz) at a resting membrane potential of −64 and −80 mV (bold trace) are shown. *c*, The effect of the NMDA-receptor channel blocker APV (100 μM) on local dendritic spikes evoked by focal synaptic stimulation to a basal dendrite. Voltage traces in control conditions and after application of APV are shown for the same synaptic stimulus intensity (2 stimuli at 50 Hz). After significantly increasing the stimulus intensity (2-fold) in the presence of APV, local fast spikes could be reinitiated (APV-strong). Note that APV abolished the slow component of the spike. Consecutive addition of CNQX (10 μM) to the APV-containing bath solution eliminated altogether the voltage response (CNQX+APV). *d*, Top panel presents the peak amplitudes of the postsynaptic voltage responses plotted as a function of the synaptic stimulus intensities at resting membrane potential (●, −64 mV) and at hyperpolarized membrane potential (◇, −80 mV). The data presented are from the same neuron as in *a*. Bottom panel shows the peak amplitudes of the postsynaptic responses plotted as a function of the synaptic stimulus intensities under control conditions (●) and in the presence of the NMDA-receptor blocker APV (◇). The data presented are from the same neuron as in *c*. *e*, The effect of carbenoxolone (100 μM) on the local dendritic spike. Black trace = control; gray trace in the presence of carbenoxolone. *f*, The spatial spread of calcium transients evoked by a local basal spike. The cell was loaded with OGB-1 (200 μM) via the somatic patch electrode. Focal stimulation to a distal basal branch (marked by the electrode drawing; scale bar, 25 μm) evoked a local basal spike composed of early fast and later slow components. Calcium fluorescence imaging was performed in the line-scan mode. Slant line scans (512 Hz time resolution) covering at least 30 μm of a basal branch at a single scan were performed. Calcium transients were analyzed off-line and presented as $\Delta F/F$ in percentage values. The calcium transients were measured from all regions of the dendritic basal branches shown, but for simplicity, only calcium transients in representative locations are shown. Note the marked decline in calcium transients along the activated basal branch, and the very small calcium transients evoked by local basal spikes in the mother and sister dendritic branches.

basal branch and extended only slightly beyond a branch point to the mother or sister branches ($n = 5$) (Wei et al., 2001). Hence, the propagation of local basal spikes was limited to a single dendritic branch, allowing for parallel nonlinear dendritic integration compartments.

To investigate the ionic mechanisms underlying both components of local basal spikes, we used UV–laser-induced focal glutamate uncaging on basal dendrites of CA1 hippocampal pyramidal neurons. Focal glutamate uncaging initiated local basal spikes, which were also composed of early fast and late slow components (Fig. 3*a*). The relative size of the late slow component was larger than that recorded for synaptic stimulation. This was probably caused by two main factors. First, glutamate uncaging preferentially activated NMDA over AMPA receptors. In addition, clearance of the uncaged glutamate is slower than synaptically released glutamate (Schiller et al., 1998). Addition of the sodium channel blocker TTX (1 μM) eliminated both spike components ($n = 5$); however, after a further increase in the laser intensity, spikes composed solely of the slow component were reinitiated in the presence of TTX, or combination of TTX and the calcium channel blocker cadmium (100 μM) (Fig. 3*b*) ($n = 3$). Similarly, addition of the NMDA-receptor blocker APV (100 μM) eliminated both spike components (Fig. 3*c*) ($n = 3$); however, after a further increase in the laser intensity, isolated fast sodium-dependent spikes were reinitiated ($n = 2$). These findings indicated that the two components of local CA1 basal spikes were mediated by different ionic mechanisms. The early fast component represented a local dendritic sodium spike, whereas the later slow component represented a local dendritic NMDA spike similar to the one described in basal dendrites of layer 5 pyramidal neurons (Schiller et al., 2000).

We next investigated the impact of fast basal spikes on the temporal accuracy of the neuronal output. On repeated identical trials, initiation of axonal action potentials showed temporal variability. We compared this temporal variability under two experimental conditions: pairing of distributed apical EPSPs with either distributed basal EPSPs or local basal spikes (Fig. 4*a*) (for details, see Materials and Methods). After repeated trials ($n = 20$) in which distributed basal and apical EPSPs were paired to produce axonal action potentials with initiation reliability of 80%, the average time delay for initiation was 7.73 ± 1.90 msec, and the average jitter of action potential timing was 1.65 ± 1.02 msec (Fig. 4*b*,*c*) ($n = 12$ neurons; SD represents the variability in the different neurons). Temporal jitter was defined as the SD of the axonal action potential timing in repeated identical trials (Mainen and Sejnowski, 1995). Fast basal spike initiation markedly improved the temporal accuracy of the output action potentials. When distributed apical EPSPs were paired with local basal spikes to produce a similar axonal action potential initiation reliability (80%), the average time delay to the action potential decreased to 4.39 ± 0.72 msec, and the temporal jitter was reduced to 0.25 ± 0.15 msec (Fig. 4*b*,*c*) ($n = 14$; $p < 0.0001$ as compared with pairing of distributed apical and basal EPSPs).

The average timing and temporal jitter of axonal action potentials evoked by pairing of distributed basal and apical EPSPs depended on the activation intensity. Increasing the activation intensity of the distributed apical EPSP (quantified by the initiation reliability of axonal action potentials) decreased the time delay and temporal jitter of axonal action potentials (Fig. 5). When action potential initiation reliability increased from 20 to 100%, the average initiation timing decreased from 8.81 ± 2.23 to 5.94 ± 1.3 msec, and the temporal jitter decreased from 1.83 ± 0.55 to 0.87 ± 0.34 msec ($n = 6$; $p < 0.01$). This reduction

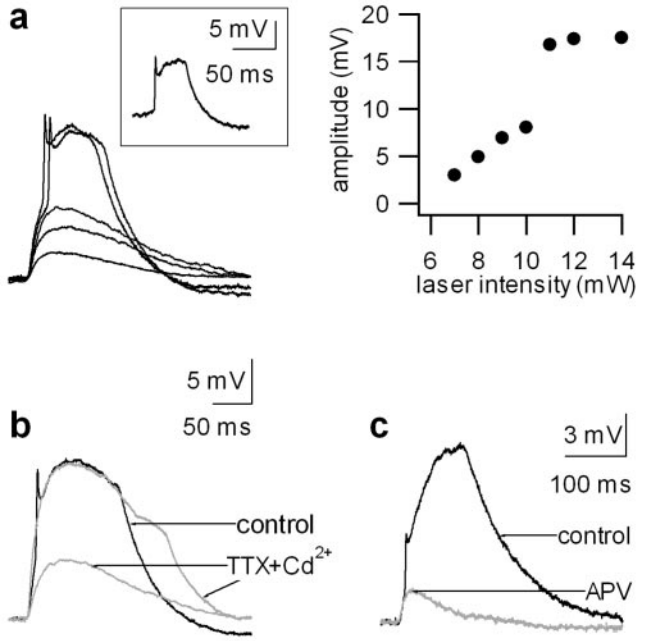

Figure 3. The ionic mechanism of the fast and slow components of local spikes in basal dendrites. A CA1 pyramidal neuron was filled with CG-1, and glutamate was uncaged via a UV laser at distal basal dendrites. *a*, Single traces of excitatory, postsynaptic-like potentials (EPSLPs) evoked by UV–laser-induced glutamate uncaging at increasing UV–laser intensities (left panel). The inset in the frame represents the net spike calculated by subtraction of the just subthreshold response from the just suprathreshold response. The peak EPSLP responses were plotted as a function of the laser intensity (right panel). *b*, Single traces of EPSLPs recorded under control conditions (black) and after the addition of TTX (1 μM) and cadmium (100 μM) (gray traces). The black and smaller gray traces were evoked by similar laser intensity (12 mW), whereas the larger gray trace was evoked by larger laser intensity (25 mW). Addition of TTX and cadmium blocked at first the fast and slow components of the local basal spikes; however, after further increasing the laser intensity (from 12 to 25 mW), reinitiation of the slow NMDA spike occurred in the presence of TTX and cadmium. *c*, Single traces of EPSLPs recorded under control conditions (black trace) and after the addition of the NMDA-receptor blocker APV (100 μM; gray trace).

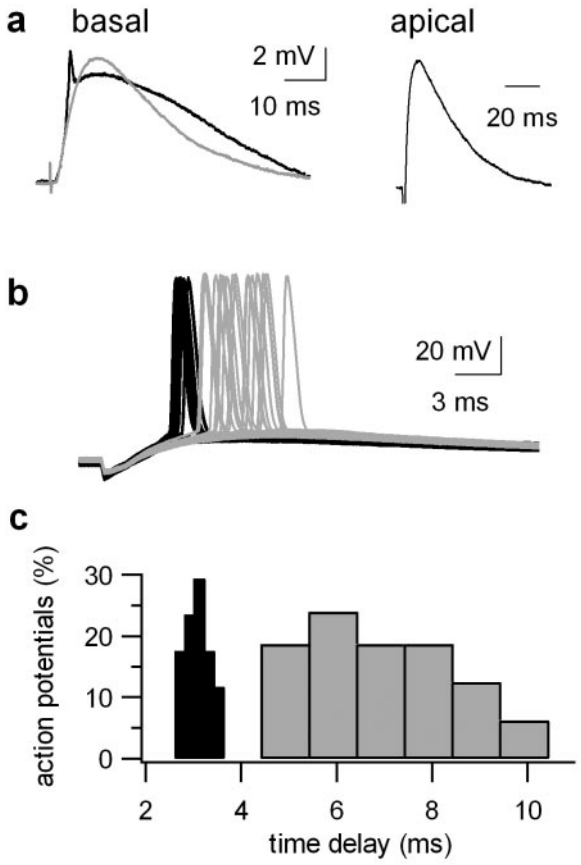

Figure 4. The effect of local fast basal spikes on the timing and temporal jitter of axonal action potentials. *a*, Single representative voltage traces of a basal EPSP (gray) and a local basal fast spike (black) that were coincidently activated with an apical EPSP. *b*, Single traces of 20 consecutive runs evoked by paired activation of a distributed apical EPSP with either a distributed basal EPSP (gray) or a local basal spike (black). The 20 consecutive stimulations were given every 20 sec. The stimulus intensity of the apical electrode was set to a level in which 10–20% of the trials failed to initiate action potentials. *c*, The timing of the axonal action potentials was monitored for each run and plotted in a time-delay histogram for the paired activation of distributed apical and basal EPSPs (gray) and distributed apical EPSPs with a local fast basal spike (black). The time delays were measured between the stimulation artifact and the peak of the action potential.

probably resulted from the fact that as the amplitude of summed somatic EPSP increased, it reached the axonal threshold earlier and with greater temporal reliability. In contrast, fast basal spikes produced a fundamentally different behavior. Both the timing and temporal jitter of the output axonal action potentials remained constant over a wide range of activation intensities. In the presence of local basal spikes, the average timing of axonal action potential at initiation reliability values of 20 and 100% were 5.0 ± 0.1 and 5.1 ± 0.1 msec, and the corresponding temporal jitters were 0.14 ± 0.02 and 0.12 ± 0.05 msec ($n = 5$) (Fig. 5). Moreover, in our experiments the temporal jitter obtained with fast basal spikes was always smaller than that obtained with distributed EPSPs, despite the fact that, in some cases, at high enough activation intensities the time delay of axonal action potentials was smaller for distributed EPSPs (Fig. 5*b*, left outermost points in top panel).

We next used computer simulations to examine the impact of fast basal spikes on the timing and precision of the neuronal output. In these simulations we compared the timing and temporal jitter of output action potentials in conditions in which the basal dendritic tree was either passive or active at different background synaptic noise. In this manner we were able to examine directly the impact of fast basal spikes on the temporal precision of output axonal action potentials. We constructed a detailed, realistic model of a CA1 pyramidal neuron in which we were able to reproduce the somatic appearance of action potentials, synaptic potentials, and fast basal spikes obtained in our experiments. The neuron was activated by 100–800 excitatory inputs distributed randomly in both the basal and apical trees paired with five inputs clustered spatially onto a single basal branch (Fig. 6*a*). The various inputs were activated within a 1 msec time window. The synaptic background activity noise in this model was produced by an additional 0–1500 inputs that were distributed randomly and activated arbitrarily along the apical tree with a frequency of 10 Hz. Each of these inputs could be either excitatory or inhibitory, with a probability of 0.7 and 0.3, respectively (Bernander et al., 1991).

Our computer simulation data confirmed the experimental findings. In contrast to the passive basal dendrites scenario in which the timing and temporal jitter of output action potentials were highly dependent on the number of activated synapses, in the neuron containing active basal dendrites, fast basal spikes preserved consistent and precise timing of output action potentials regardless of the number of coactivated distributed apical synapses (Fig. 6*d*).

In addition we examined in our simulations the effect of back-

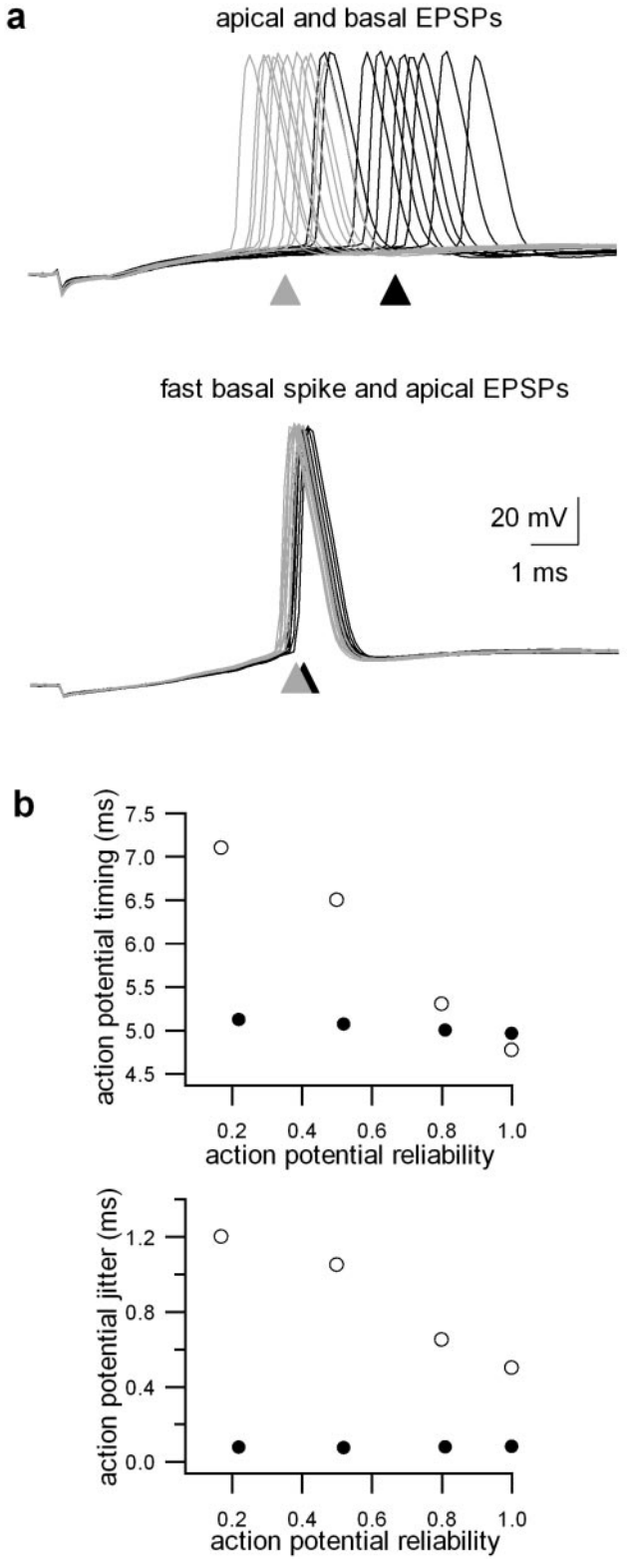

Figure 5. The impact of the activation intensity on the jitter and timing of output axonal action potentials. *a*, Pairing of basal with apical EPSPs (top traces) was compared with pairing of fast basal spikes with apical EPSPs (bottom traces). Pairing was performed at different stimulation intensities of the apical inputs, yielding different reliability values of axonal action potential initiation (reliability was defined as the fraction of traces resulting in action potential initiation). Consecutive successful runs resulting in action potential initiation are presented for two reliability values (100% gray and 20% black). Traces that failed to initiate action potentials were omitted. Arrowheads indicate the average timing of axonal action potentials in the two stimulation intensities. *b*, Action potential timing (top panel) and jitter (bottom panel) are plotted as a function of action potential reliability. The jitter was measured by the SD of action potential timing in consecutive runs. Black dots represent pairing with fast basal spikes, and open circles represent pairing with basal EPSPs. Note that the timing and jitter of axonal action potentials in the case of the fast spike was independent of the activation intensity.

ground synaptic noise on the output temporal precision with and without fast basal spikes. In the neuron with passive basal dendrites, increasing the background synaptic noise by increasing the number of arbitrarily activated apical inputs markedly impaired the precision of output action potentials (Fig. 6*d*). In contrast, fast basal spikes maintained submillisecond temporal jitter of output action potentials, despite the growing background synaptic noise (Fig. 6*d*). Hence, the effect of the fast spike on the jitter of axonal action potential timing is expected to be accentuated under *in vivo* conditions, in which the ongoing background synaptic activity is increased compared with the brain slice preparation (Bernander et al., 1991; Arieli et al., 1996; Azouz and Gray, 1999; Kamondi et al., 1998; Pare et al., 1998; Destexhe and Pare, 1999; Ho and Destexhe, 2000).

Discussion

In this paper we describe fast local spikes in CA1 basal dendrites that can transform coincidently activated input information into temporally precise and stable output information over a wide range of activation intensities and background synaptic noise. In fact, this mechanism allows activated basal inputs to serve as accurate and stable "timers" determining the temporal pattern of the neuronal output. This cellular mechanism, together with additional network mechanisms (Marsalek et al., 1997), can serve as the substrate for accurate and reliable temporal coding of information within the cortical network.

Previous studies described local dendritic spikes in apical dendrites of neocortical and hippocampal pyramidal neurons and in basal dendrites of layer 5 pyramidal neurons (Hausser et al., 2000; Schiller and Schiller, 2001). In this study we show that basal dendrites of CA1 neurons can also support initiation of local spikes, consisting of an early large fast sodium spike and a late smaller NMDA spike. Initiation of these spikes requires coincident clustered activation of inputs innervating the same dendritic segment [see modeling paper by Mel (1993)]. The number of clustered inputs required to be coincidently activated for local spikes to initiate in basal dendrites of CA1 neurons is still unknown. It should be noted that Williams and Stuart (2002) estimated that 4–30 apical inputs are needed for initiation of calcium spikes in the distal apical dendrites of layer 5 pyramidal neurons.

Here we report that these local basal spikes markedly sharpen the rising phase of EPSPs, as recorded at the soma, and as a result, critically influence the precision and reliability of output axonal action potentials. In contrast to the fast spikes described here, apical calcium spikes and basal NMDA spikes are relatively slow events and hence are unlikely to sharpen the rising phase of EPSPs (Schiller et al., 1997, 2000; Larkum et al., 1999). Previously described apical dendritic sodium spikes, which are sharp events locally, have been shown to markedly attenuate and slow down as they spread to the soma and did not contribute significantly to the rising phase of EPSPs (Schwindt and Crill, 1995; Stuart et al., 1997; Golding and Spruston, 1998); however, the reflection of local spikes at the soma is a complicated function of the passive filtering and active propagation of the signal toward the soma. It is possible that under certain conditions fast local apical spikes may also sharpen the rise time of somatic responses and contribute to output precision (Golding et al., 2002). Thus, the impact of

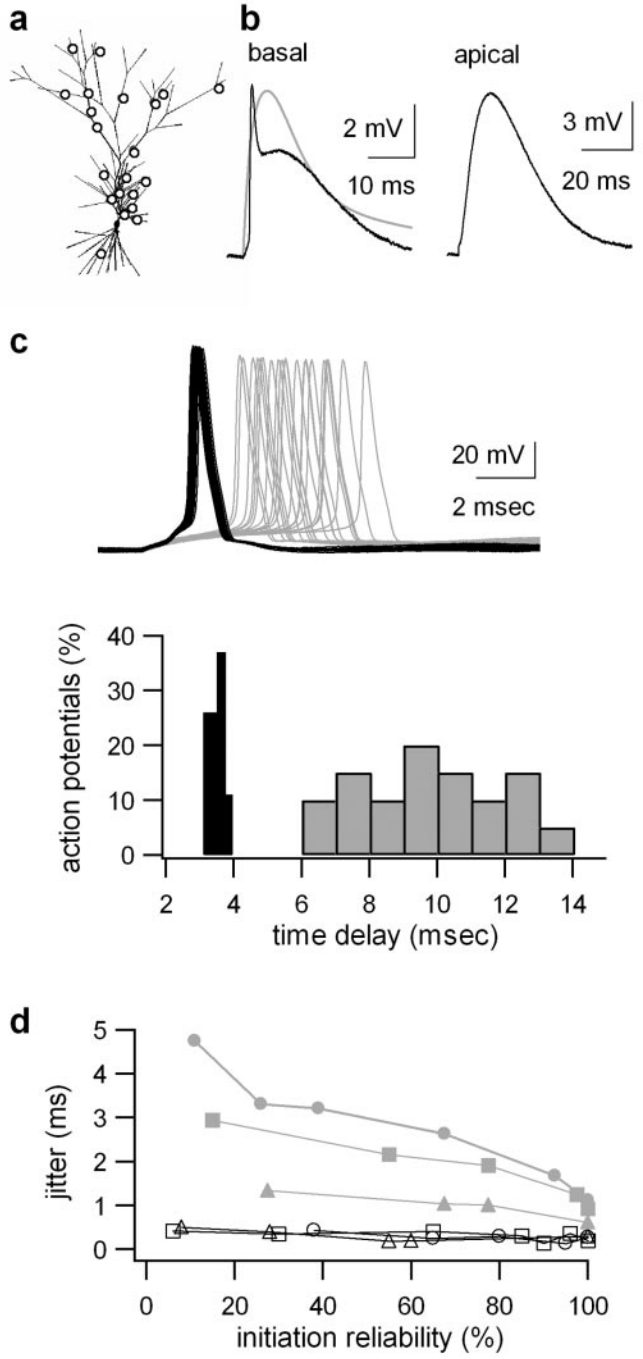

Figure 6. The effect of local fast basal spikes on the temporal jitter of axonal action potentials: computer simulation data. *a*, A CA1 pyramidal neuron was reconstructed and the responses were simulated with the NEURON software. This panel shows the reconstructed neuron, 20 of 100–800 randomly distributed apical inputs (open circles), and the basal inputs that produced the fast spike (single open circle in basal region). The reconstructed neuron was kindly provided by Dr. Guy Major. *b*, Single representative voltage traces of a basal EPSP (gray, left panel) and a local basal fast spike (black, left panel) that were coincidently activated with an apical EPSP (right panel). *c*, Top panel, Consecutive activation of randomly distributed apical inputs paired with either randomly distributed basal inputs (gray) or a local basal spike (black) to produce a reliability value of 80% in action potential initiation. Bottom panel, A time-delay histogram is plotted for the paired activation of distributed apical and basal EPSPs (gray) and distributed apical EPSPs with a local fast basal spike (black). *d*, The action potential jitter is plotted as a function of action potential reliability values at different background synaptic noise in two conditions: paired activation of distributed apical and basal EPSPs (gray) and distributed apical EPSPs with a fast basal spike (black). To achieve different synaptic baseline noises, the number of arbitrarily activated synapses was changed (circles, 1500; squares, 1000; triangles, 0 synapses). Note the constant low jitter in the case of the fast basal spike activation.

fast dendritic spikes may be a general phenomenon and not limited only to basal dendrites of CA1 neurons.

We show that coincidence detection is facilitated by fast spiking mechanisms in basal dendrites of CA1 pyramidal neurons. These findings are in contrast to previous studies by Cash and Yuste (1999), which reported linear or sublinear summation of coincidently activated inputs in CA1 neurons, but are in line with recently published studies on neocortical neurons (Larkum et al., 1999; Oviedo and Reyes, 2002; Williams and Stuart, 2002). The present results, as well as those by Williams and Stuart (2002), confirm that to achieve coincidence detection at the input level, closely spaced synapses have to be activated within a narrow time window.

It should be noted that Williams and Stuart (2002) counted the number of axonal action potentials evoked by apical calcium spikes but did not measure their temporal jitter. Thus, the question of output precision evoked by apical calcium spikes remains open. In fact, in contrast to fast basal spikes, dendritic calcium spikes in layer 5 neurons are probably imprecise output timers because they contribute a late slow voltage component to the somatic response (Softky, 1994; Schiller et al., 1997; Larkum et al., 1999).

In this study we show experimentally for the first time an active dendritic mechanism that can markedly improve the temporal precision and stability of output axonal action potentials by contributing large fast voltage transients at the soma.

Large, rapid fluctuations in somatic voltage have been recognized in the past to contribute to precise axonal action potential initiation (Mainen and Sejnowski, 1995). Various potential mechanisms have been suggested to produce rapid somatic fluctuations; among them were balanced excitation and inhibition (Shadlen and Newsome, 1994; Mainen and Sejnowski, 1995), synchronous activation of a large number of distributed inputs (Stevens and Zador, 1998; Azouz and Gray, 2000) (Fig. 5), and active dendritic mechanisms (Softky, 1994). Despite the fact that three potential mechanisms can produce rapid fluctuations in somatic voltage, they differ in their computational implications. Local active dendritic mechanisms require coincidence detection of closely spaced inputs. In contrast, balanced excitation and inhibition can result in rapid voltage fluctuations at the soma without input coincidence detection (Shadlen and Newsome, 1994, 1998). Furthermore, synchronous activation of a large number of distributed inputs (Stevens and Zador, 1998) differs from active dendritic mechanisms, which only require activation of a small number of clustered inputs.

The findings in this study show experimentally the feasibility of the third mechanism in CA1 neurons *in vitro*. Fast basal spikes are unique in their capability to preserve initiation of axonal action potentials within the same narrow submillisecond time window over a wide range of activation intensities and background synaptic noise. Although the temporal precision of axonal action potentials can be improved by activating a large number of distributed inputs synchronously (Fig. 5), the timing of action potentials is not constant and varies as a function of the number of activated inputs.

It is not clear whether fast local dendritic spikes occur *in vivo* and in what way they impact information processing in the hippocampus. Initiation of local spikes *in vivo* is expected to occur either if inputs carrying related information selectively innervate the same dendritic segments (Archie and Mel, 2000; Poirazi and Mel, 2001) or if the network activity is synchronized (Kamondi et al., 1998; Helmchen et al., 1999). It is interesting to note that a previous study has shown the appearance of sharp somatic

events, termed fast prepotentials, in CA1 hippocampal pyramidal neurons *in vivo* (Spencer and Kandel, 1968). Although the nature of these fast prepotentials has not been clarified, and they have been interpreted by some reports to represent gap junction-mediated action potentials in neighboring cells (MacVicar and Dudek, 1981; Valiante et al., 1995), they might well represent fast dendritic spikes as described here. In addition, direct dendritic recordings from apical dendrites of CA1 neurons *in vivo* have shown the occurrence of "small amplitude fast spikes" (Kamondi et al., 1998) that bear some similarities to the dendritic spikes that we describe here.

Temporal coding is used by various brain regions (Richmond and Optican, 1987; Vaadia et al., 1995; Riehle et al., 1997; Mechler et al., 1998). Auditory brain stem centers and motor and visual neocortical regions use temporal coding with millisecond or even submillisecond precision. Temporal coding with longer time scales has also been shown in the hippocampus *in vivo* (Harris et al., 2002; Mehta et al., 2002). Further studies are required to investigate whether the hippocampus also uses submillisecond temporal coding of information *in vivo*, and the role of fast dendritic spikes in this type of information coding.

References

Abeles M (1990) Corticonics. Cambridge, UK: Cambridge UP.

Archie KA, Mel BW (2000) A model for intradendritic computation of binocular disparity. Nat Neurosci 3:54–63.

Arieli A, Sterkin A, Grinvald A, Aertsen A (1996) Dynamics of ongoing activity: explanation of the large variability in evoked cortical responses. Science 273:1868–1871.

Azouz R, Gray CM (1999) Cellular mechanisms contributing to response variability of cortical neurons *in vivo*. J Neurosci 19:2209–2223.

Azouz R, Gray CM (2000) Dynamic spike threshold reveals a mechanism for synaptic coincidence detection in cortical neurons in vivo. Proc Natl Acad Sci USA 97:8110–8115.

Bernander O, Douglas RJ, Martin KA, Koch C (1991) Synaptic background activity influences spatiotemporal integration in single pyramidal cells. Proc Natl Acad Sci USA 88:11569–11573.

Bialek W, Rieke F (1992) Reliability and information transmission in spiking neurons. Trends Neurosci 15:428–434.

Cash S, Yuste R (1999) Linear summation of excitatory inputs by CA1 pyramidal neurons. Neuron 22:383–394.

Colbert CM, Magee JC, Hoffman D, Johnston D (1997) Slow recovery from inactivation of Na^+ channels underlies the activity-dependent attenuation of dendritic action potentials in hippocampal CA1 pyramidal neurons. J Neurosci 17:6512–6521.

deCharms RC, Zador A (2000) Neural representation and the cortical code. Annu Rev Neurosci 23:613–647.

Destexhe A, Pare D (1999) Impact of network activity on the integrative properties of neocortical pyramidal neurons in vivo. J Neurophysiol 81:1531–1547.

Destexhe A, Mainen ZF, Sejnowski TJ (1994) Synthesis of models for excitable membranes, synaptic transmission and neuromodulation using a common kinetic formalism. J Comput Neurosci 1:195–230.

Golding NL, Spruston N (1998) Dendritic sodium spikes are variable triggers of axonal action potentials in hippocampal CA1 pyramidal neurons. Neuron 21:1189–1200.

Golding NL, Staff NP, Spruston N (2002) Dendritic spikes as a mechanism for cooperative long-term potentiation. Nature 418:326–331.

Harris KD, Henze DA, Hirase H, Leinekugel X, Dragoi G, Czurko A, Buzsaki G (2002) Spike train dynamics predicts theta-related phase precession in hippocampal pyramidal cells. Nature 417:738–741.

Hausser M, Spruston N, Stuart GJ (2000) Diversity and dynamics of dendritic signaling. Science 290:739–744.

Helmchen F, Svoboda K, Denk W, Tank DW 1999) In-Vivo dendritic calcium dynamics in deep-layer cortical pyramidal neurons. Nat Neurosci 2:989–996.

Hines ML, Carnevale NT (1997) The NEURON simulation environment. Neural Comput 9:1179–1209.

Ho N, Destexhe A (2000) Synaptic background activity enhances the responsiveness of neocortical pyramidal neurons. J Neurophysiol 84:1488–1496.

Hoffman DA, Magee JC, Colbert CM, Johnston D (1997) K^+ channel regulation of signal propagation in dendrites of hippocampal pyramidal neurons. Nature 387:869–875.

Hopfield JJ (1995) Pattern recognition computations using action potential timing for stimulus representation. Nature 376:33–36.

Kamondi A, Acsady L, Buzsaki G (1998) Dendritic spikes are enhanced by cooperative network activity in the intact hippocampus. J Neurosci 18:3919–3928.

Larkum ME, Zhu JJ, Sakmann B (1999) A new cellular mechanism for coupling inputs arriving at different cortical layers. Nature 398:338–341.

Lecar H, Nossal R (1971a) Theory of threshold fluctuations in nerves. I. Relationships between electrical noise and fluctuations in axon firing. Biophys J 11:1048–1067.

Lecar H, Nossal R (1971b) Theory of threshold fluctuations in nerves. II. Analysis of various sources of membrane noise. Biophys J 11:1068–1084.

MacVicar BA, Dudek FE (1981) Post-natal development of electrophysiological properties of art cerebral cortical pyramidal neurons. J Physiol (Lond) 393:743–762.

Magee JC (1998) Dendritic hyperpolarization-activated currents modify the integrative properties of hippocampal CA1 pyramidal neurons. J Neurosci 18:7613–7624.

Magee JC (2000) Dendritic integration of excitatory synaptic input. Nat Rev Neurosci 1:181–190.

Magee J, Hoffman D, Colbert C, Johnston D (1998) Electrical and calcium signaling in dendrites of hippocampal pyramidal neurons. Annu Rev Physiol 60:327–346.

Mainen ZF, Sejnowski TJ (1995) Reliability of spike timing in neocortical neurons. Science 268:1503–1506.

Marsalek P, Koch C, Maunsell J (1997) On the relationship between synaptic input and spike output jitter in individual neurons. Proc Natl Acad Sci USA 21:735–740.

Mechler F, Victor JD, Purpura KP, Shapley R (1998) Robust temporal coding of contrast by V1 neurons for transient but not for steady-state stimuli. J Neurosci 18:6583–6598.

Mehta MR, Lee AK, Wilson MA (2002) Role of experience and oscillations in transforming a rate code into a temporal code. Nature 417:741–746.

Mel BW (1993) Synaptic integration in an excitable dendritic tree. J Neurophysiol 70:1086–1101.

Mel BW (1999) Why have dendrites? A computational perspective. In: Dendrites (Stuart G, Spruston N, Hausser M, eds), pp 271–289. New York: Oxford UP.

Poirazi P, Mel BW (2001) Impact of active dendrites and structural plasticity on the memory capacity of neural tissue. Neuron 29:779–796.

Migliore M, Shepherd GM (2002) Emerging rules for the distributions of active dendritic conductances. Nat Rev Neurosci 3:362–370.

Oviedo H, Reyes AD (2002) Boosting of neuronal firing evoked with asynchronous and synchronous inputs to the dendrite. Nat Neurosci 5:261–266.

Pare D, Shink E, Gaudreau H, Destexhe A, Lang EJ (1998) Impact of spontaneous synaptic activity on the resting properties of cat neocortical pyramidal neurons in vivo. J Neurophysiol 79:1450–1460.

Rall W, Segev I (1987) Functional possibilities for synapses on dendrites and on dendritic spines. In: Synaptic function (Edelman G, Gall W, Cowan W, eds), pp 605–636. New York: Wiley.

Reyes A (2001) Influence of dendritic conductances on the input-output properties of neurons. Annu Rev Neurosci 24:653–675.

Richmond BJ, Optican LM (1987) Temporal encoding of two-dimensional patterns by single units in primate inferior temporal cortex. II. Quantification of response waveform. J Neurophysiol 57:147–161.

Richmond BJ. Optican LM. Podell M, Spitzer H (1987) Temporal encoding of two-dimensional patterns by single units in primate inferior temporal cortex. I. Response characteristics. J Neurophysiol 57:132–146.

Riehle A, Grun S, Diesmann M, Aertsen A (1997) Spike synchronization and rate modulation differentially involved in motor cortical function. Science 278:1950–1953.

Rieke F, Warland D, Bialek W (1997) Spikes: exploring the neural code. Cambridge, MA: MIT.

Roelfsema PR, Engel AK, Konig P, Singer W (1997) Visuomotor integration is associated with zero time-lag synchronization among cortical areas. Nature 385:157–161.

Schiller J, Schiller Y (2001) NMDA receptor-mediated dendritic spikes and coincident signal amplification. Curr Opin Neurobiol 11:343–348.

Schiller J, Schiller Y, Stuart G, Sakmann B (1997) Calcium action potentials restricted to distal apical dendrites of rat neocortical pyramidal neurons. J Physiol (Lond) 505:605–616.

Schiller J, Schiller Y, Clapham DE (1998) NMDA receptors amplify calcium influx into dendritic spines during associative pre- and postsynaptic activation. Nat Neurosci 1:114–118.

Schiller J, Major G, Koester HJ, Schiller Y (2000) NMDA spikes in basal dendrites of cortical pyramidal neurons. Nature 404:285–289.

Schmitz D, Schuchmann S, Fisahn A, Draguhn A, Buhl EH, Petrasch-Parwez E, Dermietzel R, Heinemann U, Traub RD (2001) Axo-axonal coupling. A novel mechanism for ultrafast neuronal communication. Neuron 31:831–840.

Schwindt PC, Crill WE (1995) Amplification of synaptic current by persistent sodium conductance in apical dendrite of neocortical neurons. J Neurophysiol 74:2220–2224.

Shadlen MN, Newsome WT (1994) Noise, neural codes and cortical organization. Curr Opin Neurobiol 4:569–579.

Shadlen MN, Newsome WT (1998) The variable discharge of cortical neurons: implications for connectivity, computation, and information coding. J Neurosci 18:3870–3896.

Shepherd GM, Brayton R (1987) Logic operations are properties of computer-simulated interactions between excitable dendritic spines. Neuroscience 21:151–165.

Singer W (1999) Neuronal synchrony: a versatile code for the definition of relations? Neuron 24:49–65.

Softky W (1994) Sub-millisecond coincidence detection in active dendritic trees. Neuroscience 58:13–41.

Softky WR, Koch C (1993) The highly irregular firing of cortical cells is inconsistent with temporal integration of random EPSPs. J Neurosci 13:334–350.

Spencer WA, Kandel ER (1968) Cellular and integrative properties of the hippocampal pyramidal cell and the comparative electrophysiology of cortical neurons. Int J Neurol 6:266–296.

Steinmetz PN, Manwani A, Koch C, London M, Segev I (2000) Subthreshold voltage noise due to channel fluctuations in active neuronal membranes. J Comput Neurosci 9:133–148.

Stevens CF, Zador AM (1998) Input synchrony and the irregular firing of cortical neurons. Nat Neurosci 1:210–217.

Stuart G, Schiller J, Sakmann B (1997) Action potential initiation and propagation in rat neocortical pyramidal neurons. J Physiol (Lond) 505:617–632.

Trussell LO (1999) Synaptic mechanisms for coding timing in auditory neurons. Annu Rev Physiol 61:477–496.

Vaadia E, Haalman I, Abeles M, Bergman H, Prut Y, Slovin H, Aertsen A (1995) Dynamics of neuronal interactions in monkey cortex in relation to behavioral events. Nature 373:515–518.

Valiante TA, Velazquez JLP, Jahromi SS, Carlen PL (1995) Coupling potentials in CA1 neurons during calcium-free induced field burst activity. J Neurosci 15:6946–6956.

Van Vreeswijk C, Sompolinsky H (1998) Chaos in neuronal networks with balanced excitatory and inhibitory activity. Science 274:1724–1726.

Wei D-S, Mei Y-A, Bagal A, Kao JPY, Thompson SM, Tang C-M (2001) Compartmentalized and binary behavior of terminal dendrites in hippocampal pyramidal neurons. Science 293:2272–2275.

Williams SR, Stuart GJ (2002) Dependence of EPSP efficacy on synapse location in neocortical pyramidal neurons. Science 295:1907–1910.